

Dependence on Humidity and Aerosol Composition of the Gas-particle Partitioning of Weakly and Moderately Polar VOCs

Jeonghyeon Ahn¹, Guiying Rao¹, Eric P. Vejerano^{1*}

Center for Environmental Nanoscience and Risk, Department of Environmental Health Sciences, University of South Carolina, Columbia, SC 29208, USA

ABSTRACT

Volatile organic compounds (VOCs) dominate the class of pollutants that accumulate in the atmosphere and indoors. Assessing the gas-particle partitioning of VOCs is important to determine their fate, transport, and adverse health impacts. This work is a companion to our earlier study on the temperature dependence of VOC partitioning. Here, we report our measurement of the gas-particle partition coefficient (K_p) for weakly polar (trichloroethylene, TCE) and moderately polar (*n*-butanol, *n*-BuOH) VOCs under varying relative humidity (RH) levels onto organic and inorganic aerosols. K_p of TCE was four to five orders of magnitude lower than those of *n*-BuOH. Results suggest preferential sorption of the VOCs onto inorganic aerosol particles than onto organic aerosol particles. K_p values for both TCE and *n*-BuOH decreased as RH levels increased; the K_p for both VOCs declined sharply at an RH > 35% onto inorganic aerosol particles, whereas the K_p declined slowly onto organic aerosol particles. Partitioning of the VOCs onto organic aerosol particles was less dependent on RH levels while partitioning onto inorganic aerosol particles was important only at low RH levels. At lower RH, partitioning proceeded by adsorbing onto the aerosol particles. In contrast, at higher RH, the extremely low mass fraction of the VOCs, absorbed onto the aerosol particle's bulk by dissolving into the aqueous phase. For organic aerosol particles, partitioning may be dominated by adsorption at all RH levels. At increasing RH levels, both VOCs partitioning onto in/organic aerosol particles exhibited similar behavior (exponential) consistent to those observed for 1,2-dichlorobenzene, therefore, insensitive to the polarity. However, at a similar RH level, polarity affects the mass fraction of the VOCs that sorbed onto the aerosol particles.


Keywords: Butanol, Trichloroethylene, Emission, Organics, Deliquescence, Adsorption, Absorption

OPEN ACCESS

Received: April 21, 2021
Revised: August 6, 2021
Accepted: August 27, 2021

* **Corresponding Author:**
filonchyk.mikalai@gmail.com

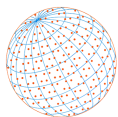
Publisher:
Taiwan Association for Aerosol
Research
ISSN: 1680-8584 print
ISSN: 2071-1409 online

 **Copyright:** The Author(s).
This is an open access article
distributed under the terms of the
[Creative Commons Attribution
License \(CC BY 4.0\)](https://creativecommons.org/licenses/by/4.0/), which permits
unrestricted use, distribution, and
reproduction in any medium,
provided the original author and
source are cited.

1 INTRODUCTION

Volatile organic compounds (VOCs) dominate the class of organic pollutants that accumulate in the atmosphere and indoors due to their low boiling point and high vapor pressure. The contribution of biogenic VOC emission from South America, which is home to the largest rainforest forest in the world, accounts for 35% of the global isoprene emission alone (Guenther *et al.*, 2012). In North America, while biogenic emissions dominate the VOC budget on a carbon basis, anthropogenic emissions comprise over half of the ambient VOC loading because of their longer aggregate lifetime (Chen *et al.*, 2019). VOC emissions from mobile sources have declined. Still, those released from volatile chemical products (VCPs) have increased (McDonald *et al.*, 2018). A primary sink of VOC is their chemical reactivity through multigenerational and multiphase reactions, converting VOCs to secondary atmospheric aerosol (SOA) (Donahue *et al.*, 2007; Gong *et al.*, 2018; Pan *et al.*, 2009).

The gas-particle partitioning coefficient (K_p) is a measure of a compound's ability to distribute between gas and aerosol phases; thus, it predicts the mobility and fate in the environment. Many

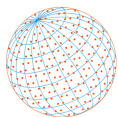


studies on contaminants in aerosols have implicated semivolatile organic compounds (SVOCs) than do VOCs since the latter do not partition preferentially onto aerosols (Liang *et al.*, 1997; Pankow, 1998; Goss and Schwarzenbach, 1999a; Qin *et al.*, 2021; Wu *et al.*, 2018). Although only a small fraction of a VOC will partition onto the gas phase, VOC concentration in the atmosphere and indoors substantially exceeds those of SVOCs (Xu and Little, 2006). Therefore, at a steady-state, for some VOCs, the mass fraction accumulated onto aerosol particles can reach similar orders to those of SVOCs (Hamilton *et al.*, 2004; Matsumoto *et al.*, 2010; Odabasi *et al.*, 2005). Assessing VOCs' gas-particle partitioning is limited by the difficulty in determining the relatively small mass fraction in the aerosol to their high gas-phase concentration. Estimates of the partitioning coefficient of VOCs have been derived mainly from field sampling. K_p acquired via field sampling can be inaccurate because of environmental and sampling factors that are difficult to control. Assessing VOCs' environmental and human health impact has been less understood because of the limited gas-particle partitioning data. To our knowledge, few studies have demonstrated the biological impact of aerosol-phase VOC. In this study, acrolein, an extremely volatile VOC, induces significant adverse biological effect on cells compared to the pristine aerosol (Ebersviller *et al.*, 2012). This study suggests the need to understand more the biological impact of aerosol-bound VOCs. Exposure to VOCs via multiple routes induces short-term and long-term adverse health effects (Brown *et al.*, 2015; Cakmak *et al.*, 2014; Gao *et al.*, 2014). Prenatal exposure to gas-phase VOCs negatively affects postnatal growth (Chang *et al.*, 2017). Even more so, aerosol-bound VOCs can reach regions of the respiratory system that are typically inaccessible to gas-phase VOCs because they are poorly absorbed by cells (Ebersviller *et al.*, 2012).

The uptake of VOCs on aerosol particles is affected by several factors. Foremost of these factors is the hygroscopic behavior and water content of aerosols. These factors are highly dependent on the chemical composition, mixing state, and RH. Here, we focus on RH and aerosol composition. The interaction of aerosol components with their surroundings is complex; changes in one property influence other physicochemical behavior (Choi and Chan, 2002; Krieger *et al.*, 2012; Martin, 2000). Uptake of water by the aerosol particles at different RH levels is a critical factor (Ding *et al.*, 2021; Hennigan *et al.*, 2009, 2008; Sun *et al.*, 2013; Zhang *et al.*, 2012). RH affects aerosol properties such as mass, size distribution, and composition (Hennigan *et al.*, 2008; Zhang *et al.*, 2012). Atmospheric aerosols of biogenic and anthropogenic origin are a mixture of complex inorganic and organic compounds with diverse physicochemical properties. Differences in composition drastically affect the partitioning behavior of a VOC on aerosol. Organic-phase water can significantly influence the total organic aerosol concentrations by increasing the aerosol mass depending on the relative humidity, particle size, and aerosol chemical composition (Jathar *et al.*, 2016; Pye *et al.*, 2017; Saxena *et al.*, 1995). Often, studies account for the impact of inorganic aerosol but neglect the contribution of organic aerosols.

The organic fraction of atmospheric aerosol contains a large amount of water-soluble organic compounds (Decesari *et al.*, 2005; Gysel *et al.*, 2004; Saxena and Hildemann, 1996). Among the most abundant is succinic acid (Kawamura and Bikkina, 2016). Ammonium sulfate and succinic acid coexist in atmospheric aerosol (Lightstone *et al.*, 2000; Liu *et al.*, 2016). The presence of water-soluble organic acid (e.g., succinic acid) can modify the phase behavior or inorganic constituent, particularly those exhibiting distinct phase transition such as ammonium sulfate (Jing *et al.*, 2018). The study outlined here focuses on aerosol with a single component (either organic or inorganic) rather than a mixture to benchmark each aerosol type's behavior under different RH levels. Although aerosols composed of a higher amount of inorganic component dictates water uptake, at an equal concentration (organic:inorganic), organic acids will influence water uptake behavior (Prenni *et al.*, 2003). Hence, for predicting water uptake on aerosol with mixed composition, data from pure components can be used, assuming that each component contributes independently (Prenni *et al.*, 2003).

Scant research was conducted on VOC partitioning onto airborne aerosol at different RH conditions. Many gas-particle partitioning studies have focused on SVOCs (Weschler and Nazaroff, 2010). SVOCs have been used as proxies in estimating the gas-particle partitioning of VOCs. However, SVOCs cannot accurately describe the VOC partitioning behavior because of the substantial differences in their physicochemical properties. Our previous study (accepted paper) investigated the partitioning behavior of 1,2-dichlorobenzene (1,2-DCB) and how temperature and RH affect partitioning. Using a previously developed method to measure the K_p of moderately



polar (*n*-butanol, *n*-BuOH), weakly polar (trichloroethylene, TCE), and nonpolar (1,2-dichlorobenzene, 1,2-DCB). This study will help understand the transport, degradation, and health impact of airborne compounds via gas-to-particle partitioning.

2 MATERIALS AND METHODS

2.1 Chemicals

For this study, we used two VOCs: *n*-BuOH ($\geq 99\%$) and TCE ($\geq 99\%$), which were purchased from Sigma Aldrich and used without further purification. We choose TCE as a surrogate for nonpolar VOCs, whereas *n*-BuOH was selected as a surrogate for moderately polar compounds. Deuterated analogs of TCE (trichloroethylene-*d*, $\geq 98\%$, Sigma-Aldrich, USA) and *n*-BuOH (1-butanol-*d*₁₀, $\geq 99\%$, Sigma-Aldrich, USA) were used as the internal standards. All solutions were prepared in methanol ($> 99.99\%$, Fisher Chemical). We generated the aerosols using dilute solutions of succinic acid ($\geq 99\%$, Alfa Aesar) and ammonium sulfate ($\geq 99\%$, Sigma). Hereafter, we will refer to aerosol particles of ammonium sulfate and succinic acid as Am Sulf and SA, respectively.

2.2 Experimental Setup

Detail of the experimental setup, characterization and verification of the total suspended particle (TSP), the analytical methods, and other important aspect of the experiment are described in our previous study (Ahn *et al.*, 2021a). Briefly, we used a cylindrical chamber ($\phi \sim 0.5$ m, $h \sim 0.1$ m, volume ~ 7 L) made of aluminum enclosed in a temperature-controlled cabinet (CEO932, LUNAIRE Environmental, New Columbia, PA) to maintain a constant temperature (Fig. 1). Three flows were directed to the chamber: dilute VOC, aerosol, and humid air flows. Dilute *n*-BuOH or TCE flow streams were generated by placing a 2-mL amber vial containing 1 mL of the pure VOC liquid in the chamber of a precision standard gas generator (491M-B, KIN-TEC Laboratories Inc, La Marque, TX, USA). Pure VOC vapor from the vial was diluted with clean, particle-free compressed air. The dilute TCE mixing ratio, or *n*-BuOH mixing ratio, was 30 ppb in air, which we used in all the tests in this study. We used a similar level for 1,2-DCB in our previous study. Mixing ratio was measured using a gas chromatograph-mass spectrometer (GC-MS) described in section 2.4. An RH/temperature probe (USBTENKI-T-RH-CC2, Dracal Technologies, Inc.) installed in the chamber measured the temperature and RH in real-time. To investigate the effect of RH on partitioning, we varied the RH level from 5% to 85%, while we maintained the temperature at 25°C. Detail of the experimental conditions is listed in Table 1.

The organic and inorganic aerosols were generated by atomizing a 200-ppm aqueous solution

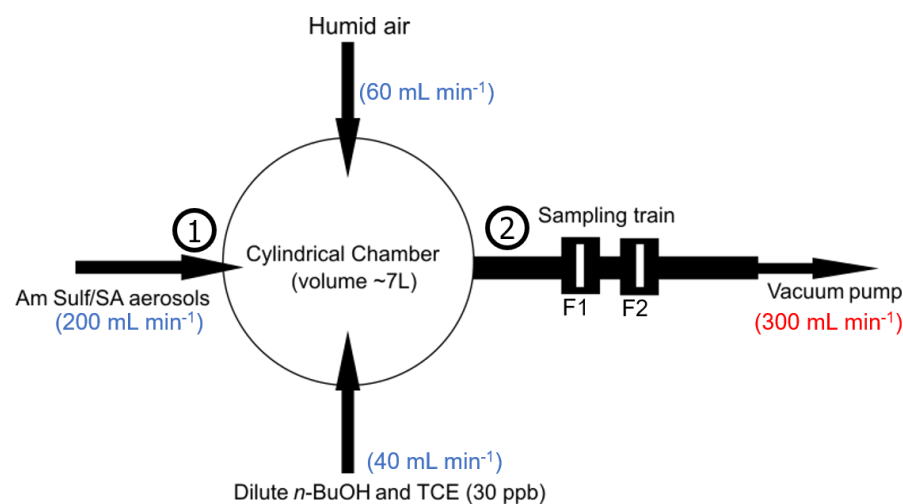
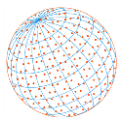


Fig. 1. The schematic of the experimental setup for measuring the gas-particle partitioning of surrogate VOCs. F1 and F2 are the filters. Location marked 1 and 2 are sites where measurement of aerosol properties was conducted. The schematic was adapted from our previous study (Ahn *et al.*, 2021a).

**Table 1.** RH levels for each compound and aerosol type used in this study.

TCE		<i>n</i> -BuOH	
Am Sulf	SA	Am Sulf	SA
5%	5%	5%	5%
35%	40%	35%	35%
55%	60%	65%	70%
85%	85%	80%	85%

of ammonium sulfate and succinic acid. Ammonium sulfate salts and organic aerosol account for > 50% of the components of atmospheric aerosols (Cass *et al.*, 2000). Ammonium sulfate is a representative of water-soluble inorganic salt, and succinic acid is a slightly water-soluble organic component in atmospheric aerosol (Abbatt *et al.*, 2005; Riipinen *et al.*, 2006). The atomizer's (TSI 3076, TSI Incorporated, Shoreview, MN) flow rate was set at 2.3 L min⁻¹ using a mass flow controller (MFC, FC-280, Tylan). Aerosol exiting the atomizer was passed through a diffusion dryer containing silica beads. Silica beads were dried by heating them at 100°C before use for each sampling. The dried aerosol was routed to the chamber at a flow rate of 200 mL min⁻¹, while the excess was vented into the atmosphere. Wet and dry air were mixed to achieve the required RH level. We set the VOC, humid air, and aerosol flow streams at 40, 60, and 200 mL min⁻¹, respectively, resulting in a total flow rate of 300 mL min⁻¹ entering the chamber. Each flow rate was optimized to minimize VOC breakthrough during the sampling. The aerosol properties were measured using a scanning mobility particle sizer (SMPS, electrostatic classifier model 3082 with a condensation particle counter model 3775, TSI Incorporated, MN).

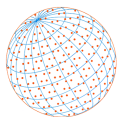
2.3 Sampling and Analysis

Two glass microfiber filters collected the aerosol containing the VOC (GF/F, ID, ~13 mm; pore size, 1.0 µm, Whatman™) embedded in a separate filter holder connected in series. The sampling flow rate was set at 300 mL min⁻¹ by an MFC with a vacuum pump (Model 6025SE-V, Environmental Monitoring System). The first filter captured the aerosol containing the sorbed VOC, whereas the second filter captured only the VOC. The second filter was used for correcting the VOC concentration in the gas phase that was collected on the filter fiber. Only a negligible amount of aerosol was captured in the second filter (Ahn *et al.*, 2021a). After sampling, each filter was transferred to 10-mL borosilicate vials to achieve equilibrium between the headspace and aerosols on the filter. To collect the VOC in the headspace at equilibrium, we used solid-phase microextraction (SPME, Supelco™) using a needle assembled with a Carboxen®/Poly-dimethylsiloxane (CAR/PDMS) fiber (Supelco™), which was inserted and suspended in the headspace for 30 min and 4 h at 22°C. The mass of VOC absorbed on SPME was injected into the GC-MS for quantitative analysis. Details of the sampling and characterization, such as the VOC recovery from the filter have been described previously (Ahn *et al.*, 2021a). Each sampling and analysis were conducted in triplicate under similar condition.

Before each sampling, the VOC was introduced into the chamber for 3 h (total chamber outflow was 300 mL min⁻¹) until the measured VOC concentration exiting the chamber was identical to that introduced. This result is consistent to the high relative recovery of VOCs from aluminum material (> 90%) stored for 48 h (Kim *et al.*, 2012), showing losses due to wall adsorption is minimal. Additionally, VOCs that sorbed on the wall equilibrated rapidly to those in the gas-phase (Shiraiwa and Seinfeld, 2012).

2.4 VOC Analysis

GC-MS (Clarus 680–Clarus SQ8T, PerkinElmer, Waltham, MA) system equipped with a DB-5 column (0.25 mm, internal diameter; 30 m, length; 0.25 µm, film thickness) was used to analyze TCE and *n*-BuOH. We used the following chromatographic condition and parameters: GC injector temperature 250°C, split flow rate 20 mL min⁻¹, carrier gas flow rate 1.1 mL min⁻¹, and carrier gas helium (99.999%). To separate TCE, we used the following GC setting: initial oven temperature 40°C, hold time 0.5 min, final temperature 100°C, ramp rate 25 °C min⁻¹. For *n*-BuOH, we used the following setting for the first ramping: initial oven temperature 40°C, hold time 0.1 min, final temperature 60°C, ramp rate 5°C min⁻¹, hold time 0.1 min. For the second ramping, the oven



temperature was set to 140°C, ramp rate 5°C min⁻¹, and hold time 0.1 min. The MS was operated under electron ionization mode at 70 eV. The spectra were acquired using selected ion monitoring. The temperature of the ion source and the transfer line were set as 200°C. Mass-to-charge ratio (*m/z*) of 130 and 132 were used to identify TCE, and *m/z* of 41 and 56 were used to identify *n*-BuOH.

2.5 K_p Calculation

The gas-particle partition coefficient, K_p , of VOCs on Am Sulf or SA aerosol particles were measured at 25°C and varying RH levels from 5 to 85%. The K_p values were calculated using the determined VOC concentration in the particle and gas phases using Eq. (1).

$$K_p = \frac{[VOC]_p}{[VOC]_g \times TSP} \quad (1)$$

where $[VOC]_p$ and $[VOC]_g$ are the VOC concentration in particle and air phases ($\mu\text{g m}^{-3}$), and TSP denotes the mass concentration of the aerosols ($\mu\text{g m}^{-3}$). We used a TSP level of $\sim 500 \mu\text{g m}^{-3}$. We used the TSP level recorded by the SMPS, which has been experimentally validated in our previous study (Ahn *et al.*, 2021a).

3 RESULTS

3.1 Effect of RH on K_p of Weakly Polar and Strongly Polar VOCs

Fig. 2 depicts the dependence of K_p with RH at a constant temperature of 25°C for TCE and *n*-BuOH partitioning onto Am Sulf aerosols. The trendlines for the K_p values for both organics decreased with increasing RH levels. For Am Sulf aerosol particles, the K_p for both *n*-BuOH and TCE were highest at a low RH and declined continuously at higher RH levels. The K_p values at an RH of $\sim 40\%$ decreased sharply for Am Sulf aerosol particles. These behaviors were similar to that of 1,2-DCB. However, compared to 1,2-DCB partitioning onto the same aerosol particles, the decline in K_p with RH was more gradual (Fig. 2). Compared to TCE and 1,2-DCB, the K_p values were higher for *n*-BuOH, suggesting that it preferentially sorbed onto Am Sulf aerosol particles.

Fig. 3 depicts the dependence of K_p with RH at a constant temperature of 25°C for TCE and *n*-BuOH partitioning onto SA aerosol particles. Compared to the partitioning of these organics onto Am Sulf aerosol particles, the K_p decline slowly with increasing RH levels. At all RH levels, the K_p varied only within an interval of $\sim 5 \times 10^{-13}$ for TCE (Fig. 3(a)) and $\sim 10 \times 10^{-13}$ for 1,2-DCB. The most extensive interval range was for *n*-BuOH, which fluctuated by an interval of $\sim 20 \times 10^{-13}$. However, compared to 1,2-DCB partitioning onto the same aerosol composition, K_p 's decline with RH was more gradual. The K_p s for *n*-BuOH were higher than those for TCE and 1,2-DCB (Figs. 2 and 3), consistent with their observed behavior on Am Sulf, suggesting preferential sorption.

Overall, the K_p s for the three VOCs partitioning into Am Sulf aerosol particles were higher than

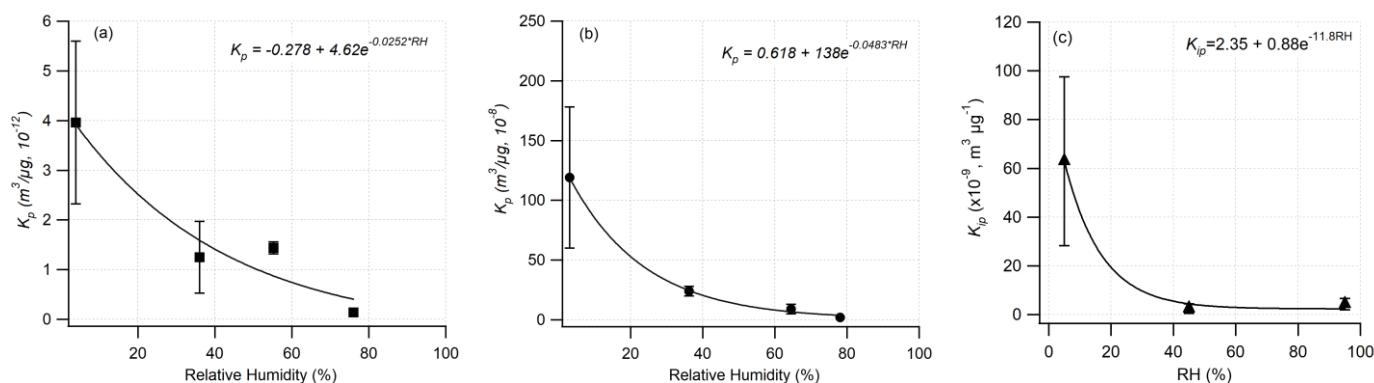


Fig. 2. The K_p of (a) TCE, (b) *n*-BuOH, and (c) 1,2-DCB (Ahn *et al.*, 2021a) partitioning into Am Sulf aerosol at 25°C at different RHs. Error bars are one standard deviation from the mean, which were taken from triplicate measurements.

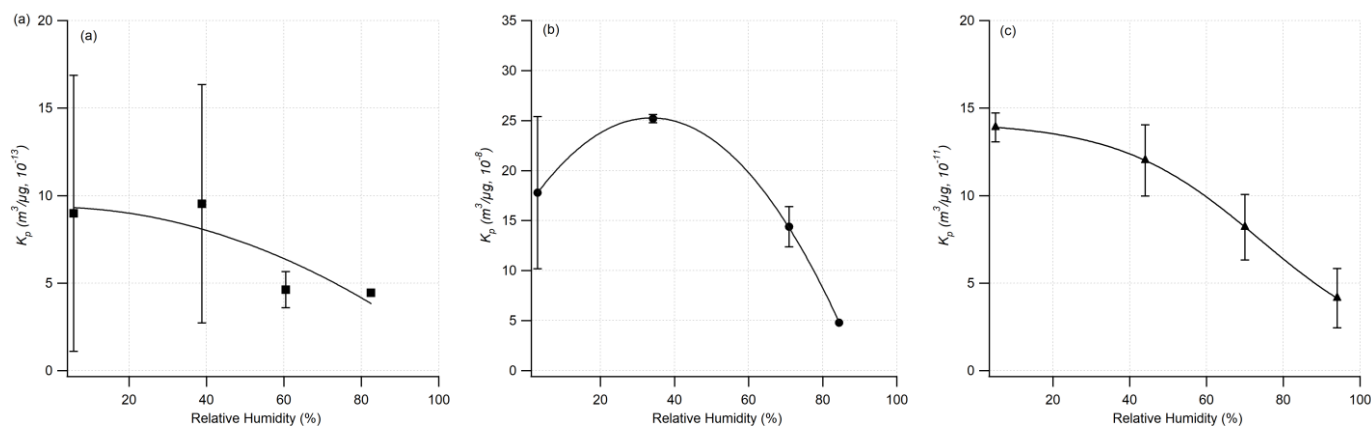
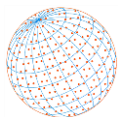


Fig. 3. The K_p of (a) TCE and (b) n -BuOH, and (c) 1,2-DCB (Ahn *et al.*, 2021a) partitioning into SA aerosol at 25°C. Error bars are one standard deviation from the mean, which were taken from triplicate measurements. Solid lines are not fit but were drawn as a guide only.

those onto SA aerosol particles. In general, the K_p for TCE, n -BuOH, and 1,2-DCB partitioning onto Am Sulf aerosol particles were $\sim 5\times$, $\sim 10\times$, and $\sim 600\times$ higher than onto SA aerosol particles. As the K_p of Am Sulf aerosol were 1.36×10^{-13} to 3.96×10^{-12} for TCE and 1.57×10^{-8} to 1.19×10^{-6} for n -BuOH, the K_p of n -BuOH was four orders of magnitude higher than those for TCE. For the partitioning onto SA aerosol particles, the K_p were 4.45×10^{-13} to 8.99×10^{-13} for TCE and 4.80×10^{-8} to 1.78×10^{-7} for n -BuOH. The K_p of n -BuOH was five orders of magnitude higher than those of TCE.

3.2 Evolution in Aerosol Properties at Different RH Levels

We monitored changes in the properties of Am Sulf and SA aerosols for ~ 8 h at different RH levels (Fig. 4). The particle median diameter appeared to be less affected by RH even at higher RH levels. The size of SA aerosol particles was slightly larger than those of Am Sulf aerosol particles; average particle median diameter was 95 ± 7 nm for Am Sulf aerosol particles and 108 ± 12 nm for SA aerosol particles. For both aerosol types, we observed that the TSP and particle number concentration fluctuated more at an RH of $\sim 85\%$ but were stable at lower RH during the 8-h monitoring. The particle number concentrations for Am Sulf aerosol were 5.37×10^6 cm $^{-3}$ at an RH of 5% RH, 5.65×10^6 cm $^{-3}$ at 35% RH, 5.48×10^6 cm $^{-3}$ at 65% RH, and 5.52×10^6 cm $^{-3}$ at 85% RH. Although the particle number concentration as depicted in Fig. 4 fluctuated the concentration remained within 10^6 cm $^{-3}$, except at an RH of 85%, which increased by an order of magnitude. Particle number concentrations of SA aerosol particles were 5.56×10^6 cm $^{-3}$, 6.24×10^6 cm $^{-3}$, 5.86×10^6 cm $^{-3}$, and 9.90×10^6 cm $^{-3}$ at RH levels of 5%, 35%, 65%, and 85%, respectively. At an RH of 85%, the number concentration for Am Sulf aerosol particles fluctuated intensely but stabilized after 4 h and resulted to higher TSP compared to those at lower RH levels. At similar RH level, the number concentration for SA aerosol particles also fluctuated for 4 h, but the TSPs were within a similar level to those measured at lower RH levels. Higher fluctuations in TSP only occurred for Am Sulf aerosol. We did not observe intense fluctuations of the TSP for SA aerosol. The TSPs measured by the SMPS were at similar levels for Am Sulf and SA aerosols, which were $1,930 \pm 461$ and $1,952 \pm 715$ $\mu\text{g m}^{-3}$, respectively. Note that the high uncertainty was due to the strong fluctuations at an RH of $\sim 85\%$. TSP and particle number concentration became slightly larger during the 8-h measurement at all RH levels.

4 DISCUSSION

Although the mass fraction of VOCs that partitions into aerosol particles is less compared to SVOCs, VOCs dominate the class of atmospheric and indoor pollutants. Therefore, some highly abundant VOC can reach concentration levels comparable to SVOCs with very low abundance (Hamilton *et al.*, 2004; Matsumoto *et al.*, 2010; Odabasi *et al.*, 2005). This companion paper

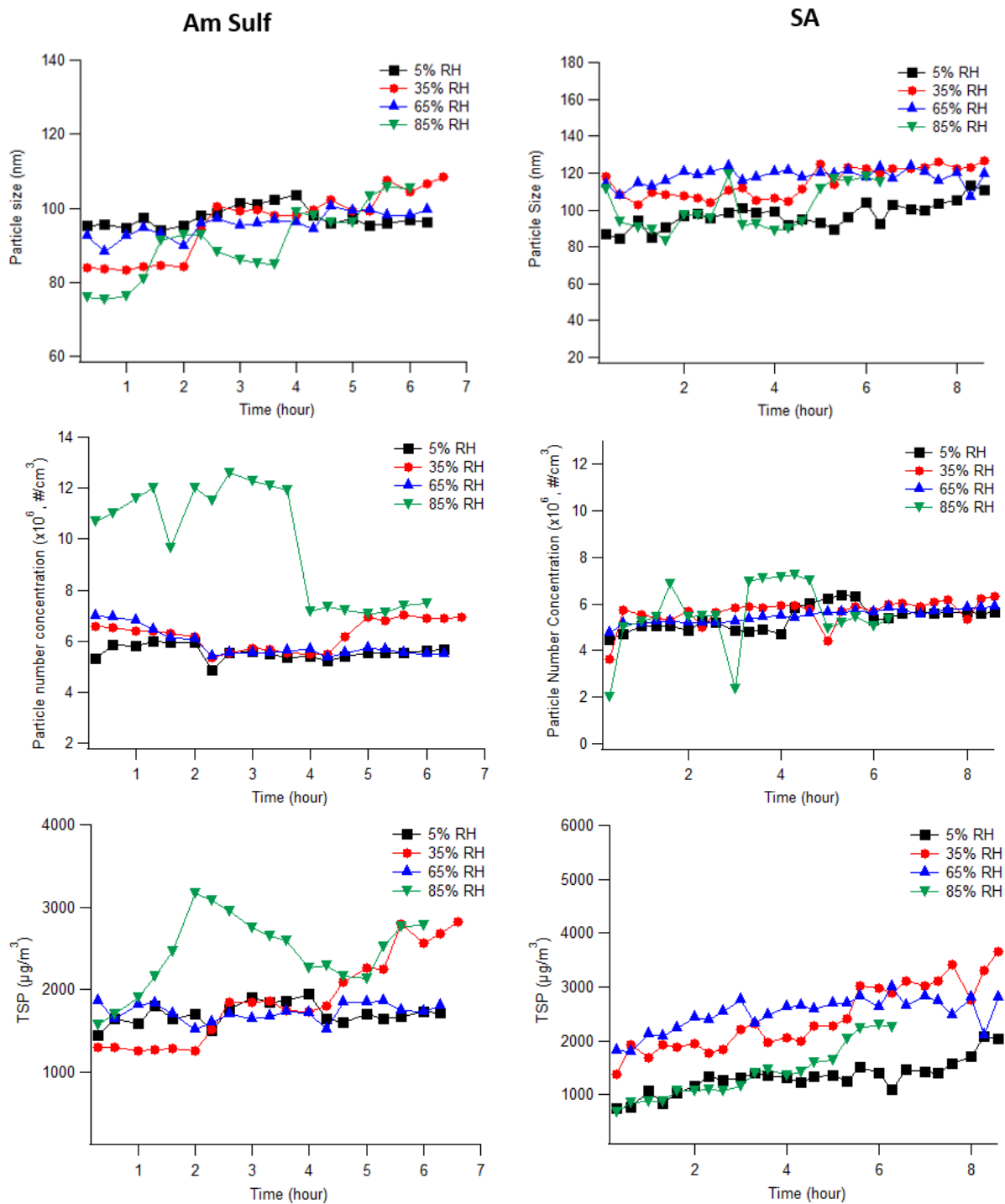
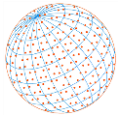
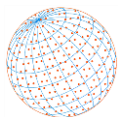


Fig. 4. Time-evolution of the particle size, particle number concentration, and TSP of Am Sulf and SA aerosols at different RH levels.

described our measurement of the partitioning coefficient for TCE and *n*-BuOH under different RH levels and aerosol composition. We compared them with our earlier studies on 1,2-DCB (Ahn *et al.*, 2021a). The K_p values for TCE and *n*-BuOH were at similar ranges to those measured for different aerosols sampled from diverse sources (Arp *et al.*, 2008) and were at similar orders to that of 1,2-DCB (Ahn *et al.*, 2021a). Overall, results showed that: (1) VOC partitioning onto Am Sulf was higher than onto SA aerosol particles; (2) partitioning on SA was affected less at all RH levels, whereas partitioning onto Am Sulf aerosol particles was affected only at low RH level.



4.1 Partitioning Mechanism

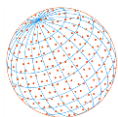
Gas-particle partitioning of organics can proceed via absorption (i.e., diffusion into the bulk of the aerosol) and adsorption (i.e., interacts with the active surface sites) (Pankow, 1994). Although the dominant partitioning mechanisms are unclear, it is well known that environmental conditions (Goss and Schwarzenbach, 1998), more importantly, RH and temperature, and aerosol composition modulate these processes. However, the effects of RH are tightly coupled with the surface chemistry of the particles (Sobanska *et al.*, 2015). In general, partitioning of the VOCs onto Am Sulf was likely via adsorption at an RH < 40%, whereas above this RH, the partitioning was more plausibly via absorption. VOC partitioning onto SA aerosols appears to proceed via adsorption at all RH levels, perhaps except at saturated RH since dried SA aerosol only deliquesces at an RH ~99% (Bilde and Svenningsson, 2004). Our earlier paper described the effects of temperature (5–35°C) for the partitioning of TCE and *n*-BuOH (Ahn *et al.*, 2021b). Partitioning of TCE is independent of temperature as deemed from the constant enthalpy of desorption consistent with the classic Vant Hoff relationship ($\ln K_p$ vs. $1/T$). However, partitioning of *n*-BuOH strongly depends on temperature, resulting in a non-linear behavior (Ahn *et al.*, 2021b). At a constant RH, but increasing temperature, absolute humidity increases; under such conditions, *n*-BuOH forms various complexes with water (DeJaco *et al.*, 2016) with different desorption enthalpies (Ahn *et al.*, 2021b).

4.2 Effect of RH

Although the fit uses at most four data points, similar to that for 1,2-DCB (Ahn *et al.*, 2021a), the partitioning of TCE and *n*-BuOH onto Am Sulf aerosol followed an exponential relationship between K_p and RH in which $\ln K_p = -C \times RH + E$, where C and E are VOC- and aerosol-specific constants (Goss, 1992; Goss and Eisenreich, 1997). For the three VOCs we studied, regardless of the polarity, RH has a negligible impact above 50%, consistent with those reported in the literature (Arp *et al.*, 2008; Cotham and Bidleman, 1992; Jathar *et al.*, 2016). The results for TCE and *n*-BuOH, and that with our previous study with 1,2-DCB, suggest that aerosol-specific properties strongly affect partitioning behavior than do VOC-specific properties. The overall K_p values of TCE and *n*-BuOH decreased as the RH increased for organic and inorganic aerosols at 25°C. However, sorption of the VOCs onto SA aerosol regardless of their polarity did not fit the exponential dependence of K_p with RH. This result suggests that partitioning behavior is driven more by aerosol-specific properties than do the VOCs' properties; under such a mechanism, it appears that the VOC's polarity has less impact on partitioning.

4.3 Effect of Water Uptake

Absorption of water has a considerable impact on partitioning. At high RH, water vapor can compete with the adsorption sites on the aerosol. At RH levels of 50 to 70%, the liquid water content of atmospheric aerosols accounts for ~10% of the total particulate mass and increases significantly at RH > 70% (Pilinis *et al.*, 1989; Thibodeaux *et al.*, 1991). For instance, organic-phase water can increase the aerosol mass, providing a larger absorbing matrix for organics (Jathar *et al.*, 2016). Am Sulf aerosol particles deliquesce at high RH (~82%) (Brooks *et al.*, 2002) and highly hygroscopic. Still, even under low RH, uptake of water can cover active sites on the aerosol particles, which will decrease the mass fraction of adsorbed organics onto the aerosol. On Am Sulf aerosol particles, partitioning is dominated primarily by the aerosol particle's higher active surface sites at low RH (adsorption) (Goss and Schwarzenbach, 1999b). On SA, water covering the active sites was less pronounced because SA is less hygroscopic than Am Sulf. Therefore, the number of active sites remained almost constant, which may explain the slow decline in K_p (Fig. 3(b)) as the RH increased. For SA aerosol particles, the dissolution of the VOCs in the aerosol water was not likely the mechanism because SA deliquesces at a high RH (Bilde and Svenningsson 2004). SA droplets do not deliquesce even at 90% RH as deemed from a single-droplet study at 25°C (Peng *et al.*, 2001). Smaller particles of SA have a higher deliquescence RH (DRH) of 99% (Bilde and Svenningsson, 2004). Moreover, the growth factor of SA (RH of 10% and 90%) was ~1, suggesting that they are not hygroscopic within this RH range (Peng *et al.*, 2001). Therefore, below saturated RH, dry SA aerosol particles introduced into the chamber was not expected to grow. However, in Fig. 4, we observed a slight change in the particle median diameter as the RH increased (Hämeri *et al.*, 2000). It is known that small soluble and insoluble particles increase in



size well below the DRH because of the adsorption of water onto their surfaces (Hämeri *et al.*, 2000). The lesser effect of RH on the K_p of the VOCs partitioning onto SA is consistent with these observations. For small Am Sulf particles, DRH is influenced by two effects. First, the solubility of a crystal increases as its size decreases, lowering the DRH. Particles smaller than 100 nm have a DRH of 79.9% (Tang and Munkelwitz, 1993). Even submicron particles of pure AS have a DRH = $80.7 \pm 0.2\%$ (Laskina *et al.*, 2015; Liu *et al.*, 2016; Wang *et al.*, 2017). Small SA particles < 200 nm require overcoming an energy barrier to uptake water (Brooks *et al.*, 2002; Wex *et al.*, 2007). Second, when the particles deliquesce, water vapor pressure increases, increasing the DRH (Hämeri *et al.*, 2000). Aerosols consisting of mixed components have significantly different DRH than aerosol consisting of single solute, such as this study. Aerosol consisting of a mixture of salts effloresces at 15–40% RH, crystallizes simultaneously, and deliquesces at 63.6% (Tang and Munkelwitz, 1993; Wu *et al.*, 2019). Thus, for a mixed aerosol, the partitioning behavior will differ from an aerosol consisting of one solute.

4.4 Effect of the VOC's Physicochemical Properties

We observed that moderately polar, weakly polar, and nonpolar aromatic VOCs have similar behavior on Am Sulf aerosol particles as shown by their trendlines in Fig. 2. However, the nature of the organics (for instance, polarity and solubility) dictates the VOC's mass fraction that will sorb onto aerosol particles. Below the DRH, aerosol particles can absorb sufficient amount of water. Hence, to some extent, the aerosol particle's surface is covered with water layers, in which the VOCs can dissolve. At higher RHs ($\geq 35\%$), the VOCs partitioned onto Am Sulf by dissolving into the aqueous phase. The amount of the VOCs that partitioned into the aerosol particles was inconsistent with the trend in water solubility of the VOCs. Although to some extent, compounds with high water solubility such as *n*-BuOH (66× higher than TCE) had a higher mass fraction partitioned onto both aerosols. However, solubility alone does not dictate mass transfer of a VOC onto aerosols. The solubility of the 1,2-DCB, TCE, and *n*-BuOH at 25°C were 1.56, 11.8, and 680 wt%, respectively. Whereas, in general, the K_p of 1,2-DCB, TCE, and *n*-BuOH at 25°C were on the order of 10^{-11} , 10^{-13} , and 10^{-8} , respectively (He *et al.*, 2010). The saturated vapor pressure, dimensionless Henry's law constant (H_L), and octanol-air partition coefficient (K_{oa}) (Table 2) of the VOCs did not result in a consistent trend with K_p . For VOCs, K_{oa} is not applicable compared to their use for predicting K_p of SVOCs. The relationship of K_p with increasing RH (i.e., being exponential) is identical for the three VOCs regardless of their polarity. However, at a similar RH level, the mass fraction that will sorb onto the aerosol particles is to some extent influenced by the VOC's polarity and their capacity to interact with the aerosol particles' active sites.

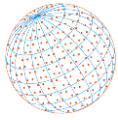
4.5 VOC/Aerosol Interactions

In general, for both aerosol types, we ascribed the larger K_p at an RH ~10%, to Van der Waals interaction between the VOC and the aerosol particles' surface. TCE, a weakly polar compound, interacts strongly with the surface of Am Sulf aerosol particles *via* Van der Waal's interaction (Schwarzenbach *et al.*, 2016), as deemed from the higher partitioning constant compared to those of SA aerosol particles. We observed a similar behavior with the other two VOCs as well. For real atmospheric aerosol consisting of hydrophobic components, this observation is applicable since nonpolar and weakly polar VOCs are less affected at RH levels of 50–90% because they preferentially partition into that phase (Cotham and Bidleman 1992; Jathar *et al.*, 2016). At low RH, TCE interacts with molecular layers of water (Goss and Schwarzenbach, 1999b), on the surface of Am Sulf aerosol *via* Van der Waal's interaction. Despite the relatively higher solubility

Table 2. Experimental and selected literature physicochemical properties of the VOCs

VOC	Experimental log K_p	Solubility (wt%)	Vapor Pressure (Torr)	Dimensionless Henry's Law Constant (H_L)	Octanol-air Partition Coefficient (K_{oa})
1,2-DCB	-11	1.56	1.36	7.8×10^{-2}	4.36
TCE	-13	11.2	69	4.2×10^{-1}	2.99
<i>n</i> -BUOH	-8	680	7	3.6×10^{-4}	4.19

Data were taken from the National Institute of Standards and Technology except the experimental log K_p .



of TCE in water to that of 1,2-DCB, the levels were similar because TCE is weakly polar and can interact with the water in the aerosol particles better by Van der Waals interaction. However, between the two types of aerosols, Van der Waals interaction of TCE with SA aerosol particles is weaker compared with Am Sulf aerosol particles.

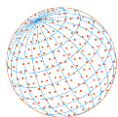
The faster decline in the K_p values even at a lower RH for Am Sulf aerosol particles is due to water film (Goss and Schwarzenbach, 1999b) covering the aerosol particles. Once the aerosol particle is covered with water the number of active sites available for the adsorption of the VOCs is reduced. At high RH, water solvates and ionizes Am Sulf aerosol. Dissolved ions interacted strongly with water, which reduced VOC uptake onto Am Sulf aerosol particles. The small mass fraction that partitioned onto the aerosol particles occurred via dissolution, the extent of which depends on the VOC's properties. However, deactivation of these sites due to water was less intense for SA aerosol particles since they deliquesce only at saturated RH. Moreover, SA aerosol particles are less hygroscopic than Am Sulf aerosol particles. Thus, at almost all RH levels, the partitioning of TCE and *n*-BuOH on SA primarily occurred *via* adsorption on the aerosol particle's surface via Van der Waals interactions (Goss, 1993; Schwarzenbach *et al.*, 2016). Of the three VOCs, *n*-BuOH had the highest K_p . This behavior is expected since *n*-BuOH can form a strong hydrogen bond with the adsorbed molecular water layer on Am Sulf or SA aerosols and with the carboxyl groups in SA. At high RH, water vapor competes strongly with *n*-BuOH for the available sorption sites on the aerosol particle's surface resulting in a slight decline in K_p .

Since we used a simple model aerosol, the interaction does not account for the complexity of aerosol systems. Ambient atmospheric aerosols contain multiple components that are susceptible to phase separate depending on the condition—more importantly—RH. Phase separation can induce the aerosol to form various structures (Freedman, 2020, 2017; You *et al.*, 2012). The formation of such structures and multiphase systems may interact with VOC differently. Hence, a model aerosol we used in this experiment will substantially exhibit drastically different partitioning behavior.

Only limited studies have assessed the health impacts of aerosol-bound VOCs, partly because of the limited data on their partitioning. VOCs' contribution in aerosol particles is often excluded in inhalation exposure assessment because it is assumed that their amount in aerosol particles is negligible. However, aerosol- and VOC-specific properties and environmental conditions affect partitioning. Thus, chronic exposure to aerosol-bound VOCs may be a significant concern depending on the VOC type and the prevailing environmental condition (e.g., RH, temperature). For example, formaldehyde is more polar and water-soluble despite being highly volatile relative to the VOCs we investigated in this study. Such a VOC class may amplify our inhalation risk because of the high mass partitioning onto aerosol particles. Our experimentally derived K_p , when coupled with particulate matter (PM) concentration data in cities worldwide and the PM fractions deposited into the different regions of the respiratory system, can be used to calculate the regional mass deposition for some VOCs. These data can be used for assessing risk and improve our knowledge of the human health impacts of aerosol-bound VOCs.

5 CONCLUSIONS

Many contaminants of concern in the environment are VOCs, which may be released into the environment from chemical spills, use and disposal of chemicals, and other activities. VOCs are subject to transfer between media. Partition coefficients are critical for predicting the fate and transport of VOCs in the environment and assessing exposure to them. In general, partitioning of the VOCs onto Am Sulf aerosol particles was likely via adsorption at an RH < 40%, whereas above this RH, the small amount detected on the aerosol potentially partitioned via absorption. On Am Sulf aerosol particles, partitioning proceeds via by adsorption due to the aerosol's higher active surface sites at low RH. It appears that aerosol-specific properties strongly affect partitioning behavior than do VOC-specific properties. For TCE, a weakly polar compound, interacted strongly with the surface of Am Sulf aerosol particles *via* Van der Waal's interaction, as deemed from the higher partitioning constant compared to those of SA aerosol particles. The faster decline in the K_p values even at a lower RH for Am Sulf aerosol particles is due to water film covering the surface and is more hygroscopic than SA aerosol particles. Deactivation of active sites by water was less intense for SA aerosol particles because they deliquesce only at nearly saturated RH. *n*-BuOH had



the highest K_p , which we attribute to its ability to form strong hydrogen bond with the adsorbed molecular water layer on both aerosols. These studies were conducted on simple model aerosols. Future studies should investigate more complex aerosols as aerosol-specific properties appear to dictate partitioning. We expect that a more complex aerosols would behave substantially different from our model aerosols. These experimental gas-particle partitioning data can be used for developing VOC-specific models. Results can be used to improve the prediction of the impacts of VOCs on health and the environment.

CONFLICTS OF INTEREST

We declare we have no conflicts of interest.

DISCLAIMER

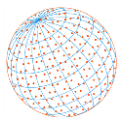
Reference to any companies or specific commercial products does not constitute endorsement by the authors.

ACKNOWLEDGEMENT

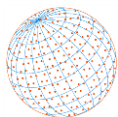
We thank the US Army Research Office (GRANT11970168) for providing financial support.

REFERENCES

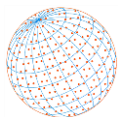
- Abbatt, J.P.D., Broekhuizen, K., Pradeep Kumar, P. (2005). Cloud condensation nucleus activity of internally mixed ammonium sulfate/organic acid aerosol particles. *Atmos. Environ.* 39, 4767–4778. <https://doi.org/10.1016/j.atmosenv.2005.04.029>
- Ahn, J., Rao, G., Vejerano, E. (2021a). Partitioning of 1,2-dichlorobenzene onto organic and inorganic aerosols. *Environ Chem.* 18, 61–70. <https://doi.org/10.1071/EN21016>
- Ahn, J., Rao, G., Vejerano, E. (2021b). Temperature dependence of the gas-particle partitioning of selected VOCs. *Environ. Sci. Processes Impacts* 23, 947–955. <https://doi.org/10.1039/D1EM00176K>
- Arp, H.P.H., Schwarzenbach, R.P., Goss, K.U. (2008). Ambient gas/particle partitioning. 1. Sorption mechanisms of apolar, polar, and ionizable organic compounds. *Environ. Sci. Technol.* 42, 5541–5547. <https://doi.org/10.1021/es703094u>
- Bilde, M., Svenningsson, B. (2004). CCN activation of slightly soluble organics: The importance of small amounts of inorganic salt and particle phase. *Tellus B* 56, 128–134. <https://doi.org/10.3402/tellusb.v56i2.16406>
- Brooks, S.D., Wise, M.E., Cushing, M., Tolbert, M.A. (2002). Deliquescence behavior of organic/ammonium sulfate aerosol. *Geophys. Res. Lett.* 29, 23-1–23–24. <https://doi.org/10.1029/2002GL014733>
- Brown, D.R., Lewis, C., Weinberger, B.I. (2015). Human exposure to unconventional natural gas development: A public health demonstration of periodic high exposure to chemical mixtures in ambient air. *J. Environ. Sci. Health., Part A* 50, 460–472. <https://doi.org/10.1080/10934529.2015.992663>
- Cakmak, S., Dales, R.E., Liu, L., Kauri, L.M., Lemieux, C.L., Hebborn, C., Zhu, J. (2014). Residential exposure to volatile organic compounds and lung function: Results from a population-based cross-sectional survey. *Environ. Pollut.* 194, 145–151. <https://doi.org/10.1016/j.envpol.2014.07.020>
- Cass, G.R., Hughes, L.A., Bhave, P., Kleeman, M.J., Allen, J.O., Salmon, L.G. (2000). The chemical composition of atmospheric ultrafine particles. *Philos. Trans. R. Soc. London, Ser. A* 358, 2581–2592. <https://doi.org/10.1098/rsta.2000.0670>
- Chang, M., Park, H., Ha, M., Hong, Y.C., Lim, Y.H., Kim, Y., Kim, Y.J., Lee, D., Ha, E.H. (2017). The effect of prenatal TVOC exposure on birth and infantile weight: The Mothers and Children's Environmental Health study. *Pediatr. Res.* 82, 423. <https://doi.org/10.1038/pr.2017.55>



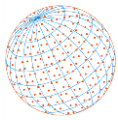
- Chen, X., Millet, D.B., Singh, H.B., Wisthaler, A., Apel, E.C., Atlas, E.L., Blake, D.R., Bourgeois, I., Brown, S.S., Crouse, J.D., de Gouw, J.A., Flocke, F.M., Fried, A., Heikes, B.G., Hornbrook, R.S., Mikoviny, T., Min, K.E., Müller, M., Neuman, J.A., O'Sullivan, D.W., *et al.* (2019). On the sources and sinks of atmospheric VOCs: An integrated analysis of recent aircraft campaigns over North America. *Atmos. Chem. Phys.* 19, 9097–9123. <https://doi.org/10.5194/acp-19-9097-2019>
- Choi, M.Y., Chan, C.K. (2002). The effects of organic species on the hygroscopic behaviors of inorganic aerosols. *Environ. Sci. Technol.* 36, 2422–2428. <https://doi.org/10.1021/es0113293>
- Cotham, W.E., Bidleman, T.F. (1992). Laboratory investigations of the partitioning of organochlorine compounds between the gas phase and atmospheric aerosols on glass fiber filters. *Environ. Sci. Technol.* 26, 469–478. <https://doi.org/10.1021/es00027a003>
- Decesari, S., Facchini, M.C., Fuzzi, S., McFiggans, G.B., Coe, H., Bower, K.N. (2005). The water-soluble organic component of size-segregated aerosol, cloud water and wet depositions from Jeju Island during ACE-Asia. *Atmos. Environ.* 39, 211–222. <https://doi.org/10.1016/j.atmosenv.2004.09.049>
- Ding, J., Dai, Q., Zhang, Y., Xu, J., Huangfu, Y., Feng, Y. (2021). Air humidity affects secondary aerosol formation in different pathways. *Sci. Total Environ.* 759, 143540. <https://doi.org/10.1016/j.scitotenv.2020.143540>
- Donahue, N.M., Tischuk, J.E., Marquis, B.J., Hartz, K.E.H. (2007). Secondary organic aerosol from limona ketone: Insights into terpene ozonolysis via synthesis of key intermediates. *Phys. Chem. Chem. Phys.* 9, 2991–2998. <https://doi.org/10.1039/B701333G>
- Ebersviller, S., Lichtveld, K., Sexton, K.G., Zavala, J., Lin, Y.H., Jaspers, I., Jeffries, H.E. (2012). Gaseous VOCs rapidly modify particulate matter and its biological effects – Part 1: Simple VOCs and model PM. *Atmos. Chem. Phys. Discuss.* 12, 5065–5105. <https://doi.org/10.5194/acpd-12-5065-2012>
- Freedman, M.A. (2017). Phase separation in organic aerosol. *Chem. Soc. Rev.* 46, 7694–7705. <https://doi.org/10.1039/C6CS00783J>
- Freedman, M.A. (2020). Liquid–liquid phase separation in supermicrometer and submicrometer aerosol particles. *Acc. Chem. Res.* 53, 1102–1110. <https://doi.org/10.1021/acs.accounts.0c00093>
- Gao, Y., Zhang, Y., Kamijima, M., Sakai, K., Khalequzzaman, M., Nakajima, T., Shi, R., Wang, X., Chen, D., Ji, X. (2014). Quantitative assessments of indoor air pollution and the risk of childhood acute leukemia in Shanghai. *Environ. Pollut.* 187, 81–89. <https://doi.org/10.1016/j.envpol.2013.12.029>
- Gong, Y., Chen, Z., Li, H. (2018). The oxidation regime and SOA composition in limonene ozonolysis: Roles of different double bonds, radicals, and water. *Atmos. Chem. Phys.* 18, 15105–15123. <https://doi.org/10.5194/acp-18-15105-2018>
- Goss, K.U. (1992). Effects of temperature and relative humidity on the sorption of organic vapors on quartz sand. *Environ. Sci. Technol.* 26, 2287–2294. <https://doi.org/10.1021/es00035a030>
- Goss, K.U. (1993). Effects of temperature and relative humidity on the sorption of organic vapors on clay minerals. *Environ. Sci. Technol.* 27, 2127–2132. <https://doi.org/10.1021/es00047a019>
- Goss, K.U., Eisenreich, S.J. (1997). Sorption of volatile organic compounds to particles from a combustion source at different temperatures and relative humidities. *Atmos. Environ.* 31, 2827–2834. [https://doi.org/10.1016/S1352-2310\(97\)00048-4](https://doi.org/10.1016/S1352-2310(97)00048-4)
- Goss, K.U., Schwarzenbach, R.P. (1999a). Quantification of the effect of humidity on the gas/mineral oxide and gas/salt adsorption of organic compounds. *Environ. Sci. Technol.* 33, 4073–4078. <https://doi.org/10.1021/es990502g>
- Goss, K.U., Schwarzenbach, R.P. (1999b). Quantification of the effect of humidity on the gas/mineral oxide and gas/salt adsorption of organic compounds. *Environ. Sci. Technol.* 33, 4073–4078. <https://doi.org/10.1021/es990502g>
- Guenther, A.B., Jiang, X., Heald, C.L., Sakulyanontvittaya, T., Duhl, T., Emmons, L.K., Wang, X. (2012). The Model of Emissions of Gases and Aerosols from Nature version 2.1 (MEGAN2.1): an extended and updated framework for modeling biogenic emissions. *Geosci. Model Dev.* 5, 1471–1492. <https://doi.org/10.5194/gmd-5-1471-2012>
- Gysel, M., Weingartner, E., Nyeki, S., Paulsen, D., Baltensperger, U., Galambos, I., Kiss, G. (2004). Hygroscopic properties of water-soluble matter and humic-like organics in atmospheric fine aerosol. *Atmos. Chem. Phys.* 4, 35–50. <https://doi.org/10.5194/acp-4-35-2004>
- Hämeri, K., Väkevä, M., Hansson, H.C., Laaksonen, A. (2000). Hygroscopic growth of ultrafine ammonium sulphate aerosol measured using an ultrafine tandem differential mobility



- analyzer. *J. Geophys. Res.* 105, 22231–22242. <https://doi.org/10.1029/2000JD900220>
- Hamilton, J.F., Webb, P.J., Lewis, A.C., Hopkins, J.R., Smith, S., Davy, P. (2004). Partially oxidised organic components in urban aerosol using GCXGC-TOF/MS. *Atmos. Chem. Phys.* 4, 1279–1290. <https://doi.org/10.5194/acp-4-1279-2004>
- He, Y., Jain, P., Yalkowsky, S.H. (2010). Handbook of aqueous solubility data. CRC press.
- Hennigan, C.J., Bergin, M.H., Dibb, J.E., Weber, R.J. (2008). Enhanced secondary organic aerosol formation due to water uptake by fine particles. *Geophys. Res. Lett.* 35, L18801. <https://doi.org/10.1029/2008GL035046>
- Hennigan, C.J., Bergin, M.H., Russell, A.G., Nenes, A., Weber, R.J. (2009). Gas/particle partitioning of water-soluble organic aerosol in Atlanta. *Atmos. Chem. Phys.* 9, 3613–3628. <https://doi.org/10.5194/acp-9-3613-2009>
- Jathar, S.H., Mahmud, A., Barsanti, K.C., Asher, W.E., Pankow, J.F., Kleeman, M.J. (2016). Water uptake by organic aerosol and its influence on gas/particle partitioning of secondary organic aerosol in the United States. *Atmos. Environ.* 129, 142–154. <https://doi.org/10.1016/j.atmosenv.2016.01.001>
- Jing, B., Wang, Z., Tan, F., Guo, Y., Tong, S., Wang, W., Zhang, Y., Ge, M. (2018). Hygroscopic behavior of atmospheric aerosols containing nitrate salts and water-soluble organic acids. *Atmos. Chem. Phys.* 18, 5115–5127. <https://doi.org/10.5194/acp-18-5115-2018>
- Kawamura, K., Bikkina, S. (2016). A review of dicarboxylic acids and related compounds in atmospheric aerosols: Molecular distributions, sources and transformation. *Atmos. Res.* 170, 140–160. <https://doi.org/10.1016/j.atmosres.2015.11.018>
- Kim, Y.H., Kim, K.H., Jo, S.H., Jeon, E.C., Sohn, J.R., Parker, D.B. (2012). Comparison of storage stability of odorous VOCs in polyester aluminum and polyvinyl fluoride Tedlar® bags. *Anal. Chim. Acta* 712, 162–167. <https://doi.org/10.1016/j.aca.2011.11.014>
- Krieger, U.K., Marcolli, C., Reid, J.P. (2012). Exploring the complexity of aerosol particle properties and processes using single particle techniques. *Chem. Soc. Rev.* 41, 6631–6662. <https://doi.org/10.1039/C2CS35082C>
- Laskina, O., Morris, H.S., Grandquist, J.R., Qin, Z., Stone, E.A., Tivanski, A.V., Grassian, V.H. (2015). Size matters in the water uptake and hygroscopic growth of atmospherically relevant multicomponent aerosol particles. *J. Phys. Chem. A* 119, 4489–4497. <https://doi.org/10.1021/jp510268p>
- Liang, C., Pankow, J.F., Odum, J.R., Seinfeld, J.H. (1997). Gas/particle partitioning of semivolatile organic compounds to model inorganic, organic, and ambient smog aerosols. *Environ. Sci. Technol.* 31, 3086–3092. <https://doi.org/10.1021/es9702529>
- Lightstone, J.M., Onasch, T.B., Imre, D., Oatis, S. (2000). Deliquescence, efflorescence, and water activity in ammonium nitrate and mixed ammonium nitrate/succinic acid microparticles. *J. Phys. Chem. A* 104, 9337–9346. <https://doi.org/10.1021/jp002137h>
- Liu, Q., Jing, B., Peng, C., Tong, S., Wang, W., Ge, M. (2016). Hygroscopicity of internally mixed multi-component aerosol particles of atmospheric relevance. *Atmos. Environ.* 125, 69–77. <https://doi.org/10.1016/j.atmosenv.2015.11.003>
- Martin, S.T. (2000). Phase transitions of aqueous atmospheric particles. *Chem. Rev.* 100, 3403–3454. <https://doi.org/10.1021/cr990034t>
- Matsumoto, K., Matsumoto, K., Mizuno, R., Igawa, M. (2010). Volatile organic compounds in ambient aerosols. *Atmos. Res.* 97, 124–128. <https://doi.org/10.1016/j.atmosres.2010.03.014>
- McDonald, B.C., de Gouw, J.A., Gilman, J.B., Jathar, S.H., Akherati, A., Cappa, C.D., Jimenez, J.L., Lee-Taylor, J., Hayes, P.L., McKeen, S.A., Cui, Y.Y., Kim, S.W., Gentner, D.R., Isaacman-VanWertz, G., Goldstein, A.H., Harley, R.A., Frost, G.J., Roberts, J.M., Ryerson, T.B., Trainer, M. (2018). Volatile chemical products emerging as largest petrochemical source of urban organic emissions. *Science* 359, 760–764. <https://doi.org/10.1126/science.aag0524>
- Odabasi, M., Ongan, O., Cetin, E. (2005). Quantitative analysis of volatile organic compounds (VOCs) in atmospheric particles. *Atmos. Environ.* 39, 3763–3770. <https://doi.org/10.1016/j.atmosenv.2005.02.048>
- Pan, X., Underwood, J.S., Xing, J.H., Mang, S.A., Nizkorodov, S.A. (2009). Photodegradation of secondary organic aerosol generated from limonene oxidation by ozone studied with chemical ionization mass spectrometry. *Atmos. Chem. Phys.* 9, 3851–3865. <https://doi.org/10.5194/acp-9-3851-2009>
- Pankow, J.F. (1994). An absorption model of the gas/aerosol partitioning involved in the formation



- of secondary organic aerosol. *Atmos. Environ.* 28, 189–193. [https://doi.org/10.1016/1352-2310\(94\)90094-9](https://doi.org/10.1016/1352-2310(94)90094-9)
- Pankow, J.F. (1998). Further discussion of the octanol/air partition coefficient K_{oa} as a correlating parameter for gas/particle partitioning coefficients. *Atmos. Environ.* 32, 1493–1497. [https://doi.org/10.1016/S1352-2310\(97\)00383-X](https://doi.org/10.1016/S1352-2310(97)00383-X)
- Peng, C., Chan, M.N., Chan, C.K. (2001). The hygroscopic properties of dicarboxylic and multifunctional acids: Measurements and UNIFAC predictions. *Environ. Sci. Technol.* 35, 4495–4501. <https://doi.org/10.1021/es0107531>
- Pilinis, C., Seinfeld, J.H., Grosjean, D. (1989). Water content of atmospheric aerosols. *Atmos. Environ.* 23, 1601–1606. [https://doi.org/10.1016/0004-6981\(89\)90419-8](https://doi.org/10.1016/0004-6981(89)90419-8)
- Prenni, A.J., DeMott, P.J., Kreidenweis, S.M. (2003). Water uptake of internally mixed particles containing ammonium sulfate and dicarboxylic acids. *Atmos. Environ.* 37, 4243–4251. [https://doi.org/10.1016/S1352-2310\(03\)00559-4](https://doi.org/10.1016/S1352-2310(03)00559-4)
- Pye, H.O.T., Murphy, B.N., Xu, L., Ng, N.L., Carlton, A.G., Guo, H., Weber, R., Vasilakos, P., Appel, K.W., Budisulistiorini, S.H., Surratt, J.D., Nenes, A., Hu, W., Jimenez, J.L., Isaacman-VanWertz, G., Misztal, P.K., Goldstein, A.H. (2017). On the implications of aerosol liquid water and phase separation for organic aerosol mass. *Atmos. Chem. Phys.* 17, 343–369. <https://doi.org/10.5194/acp-17-343-2017>
- Qin, M., Yang, P.F., Hu, P.T., Hao, S., Macdonald, R.W., Li, Y.F. (2021). Particle/gas partitioning for semi-volatile organic compounds (SVOCs) in level III multimedia fugacity models: Both gaseous and particulate emissions. *Sci. Total Environ.* 790, 148012. <https://doi.org/10.1016/j.scitotenv.2021.148012>
- Riipinen, I., Svenningsson, B., Bilde, M., Gaman, A., Lehtinen, K.E.J., Kulmala, M. (2006). A method for determining thermophysical properties of organic material in aqueous solutions: Succinic acid. *Atmos. Res.* 82, 579–590. <https://doi.org/10.1016/j.atmosres.2006.02.014>
- Saxena, P., Hildemann, L.M., McMurry, P.H., Seinfeld, J.H. (1995). Organics alter hygroscopic behavior of atmospheric particles. *J. Geophys. Res.* 100, 18755–18770. <https://doi.org/10.1029/95JD01835>
- Saxena, P., Hildemann, L.M. (1996). Water-soluble organics in atmospheric particles: A critical review of the literature and application of thermodynamics to identify candidate compounds. *J. Atmos. Chem.* 24, 57–109. <https://doi.org/10.1007/BF00053823>
- Schwarzenbach, R.P., Gschwend, P.M., Imboden, D.M. (2016). *Environmental organic chemistry*. John Wiley & Sons.
- Shiraiwa, M., Seinfeld, J.H. (2012). Equilibration timescale of atmospheric secondary organic aerosol partitioning. *Geophys. Res. Lett.* 39, L24801. <https://doi.org/10.1029/2012GL054008>
- Sobanska, S., Barbillat, J., Moreau, M., Nuns, N., De Waele, I., Petitprez, D., Tobon, Y., Bremard, C. (2015). Influence of stearic acid coating of the NaCl surface on the reactivity with NO₂ under humidity. *Phys. Chem. Chem. Phys.* 17, 10963–10977. <https://doi.org/10.1039/C4CP05655H>
- Sun, Y., Wang, Z., Fu, P., Jiang, Q., Yang, T., Li, J., Ge, X. (2013). The impact of relative humidity on aerosol composition and evolution processes during wintertime in Beijing, China. *Atmos. Environ.* 77, 927–934. <https://doi.org/10.1016/j.atmosenv.2013.06.019>
- Tang, I.N., Munkelwitz, H.R. (1993). Composition and temperature dependence of the deliquescence properties of hygroscopic aerosols. *Atmos. Environ.* 27, 467–473. [https://doi.org/10.1016/0960-1686\(93\)90204-C](https://doi.org/10.1016/0960-1686(93)90204-C)
- Thibodeaux, L.J., Nadler, K.C., Valsaraj, K.T., Reible, D.D. (1991). The effect of moisture on volatile organic chemical gas-to-particle partitioning with atmospheric aerosols—competitive adsorption theory predictions. *Atmos. Environ.* 25, 1649–1656. [https://doi.org/10.1016/0960-1686\(91\)90023-Z](https://doi.org/10.1016/0960-1686(91)90023-Z)
- Wang, X., Jing, B., Tan, F., Ma, J., Zhang, Y., Ge, M. (2017). Hygroscopic behavior and chemical composition evolution of internally mixed aerosols composed of oxalic acid and ammonium sulfate. *Atmos. Chem. Phys.* 17, 12797–12812. <https://doi.org/10.5194/acp-17-12797-2017>
- Weschler, C.J., Nazaroff, W.W. (2010). SVOC partitioning between the gas phase and settled dust indoors. *Atmos. Environ.* 44, 3609–3620. <https://doi.org/10.1016/j.atmosenv.2010.06.029>
- Wex, H., Ziese, M., Kiselev, A., Henning, S., Stratmann, F. (2007). Deliquescence and hygroscopic growth of succinic acid particles measured with LACIS. *Geophys. Res. Lett.* 34, L17810. <https://doi.org/10.1029/2007GL030185>



- Wu, L., Li, X., Ro, C.U. (2019). Hygroscopic behavior of ammonium sulfate, ammonium nitrate, and their mixture particles. *Asian J. Atmos. Environ.* 13, 196–211. <https://doi.org/10.5572/ajae.2019.13.3.196>
- Wu, Y., Eichler, C.M.A., Cao, J., Benning, J., Olson, A., Chen, S., Liu, C., Vejerano, E.P., Marr, L.C., Little, J.C. (2018). Particle/gas partitioning of phthalates to organic and inorganic airborne particles in the indoor environment. *Environ. Sci. Technol.* 52, 3583–3590. <https://doi.org/10.1021/acs.est.7b05982>
- Xu, Y., Little, J.C. (2006). Predicting emissions of SVOCs from polymeric materials and their interaction with airborne particles. *Environ. Sci. Technol.* 40, 456–461. <https://doi.org/10.1021/es051517j>
- You, Y., Renbaum-Wolff, L., Carreras-Sospedra, M., Hanna, S.J., Hiranuma, N., Kamal, S., Smith, M.L., Zhang, X., Weber, R.J., Shilling, J.E., Dabdub, D., Martin, S.T., Bertram, A.K. (2012). Images reveal that atmospheric particles can undergo liquid-liquid phase separations. *Proc. Natl. Acad. Sci. U.S.A.* 109, 13188–13193. <https://doi.org/10.1073/pnas.1206414109>
- Zhang, X., Liu, J., Parker, E.T., Hayes, P.L., Jimenez, J.L., Gouw, J.A. de, Flynn, J.H., Grossberg, N., Lefer, B.L., Weber, R.J. (2012). On the gas-particle partitioning of soluble organic aerosol in two urban atmospheres with contrasting emissions: 1. Bulk water-soluble organic carbon. *J. Geophys. Res.* 117, D00V16. <https://doi.org/10.1029/2012JD017908>